Integrated high-temperature piezoelectric plate acoustic wave transducers using mode conversion

Wu, K.-T.; Kobayashi, M.; Jen, C.-K.

Publisher's version / la version de l'éditeur:
IEEE Transactions on Ultrasonics, Ferroelectrics and Frequency Control, 56, 6, pp. 1218-1224, 2009-06

Web page / page Web
http://dx.doi.org/10.1109/TUFFC.2009.1163
http://nparc.cisti-icist.nrc-cnrc.gc.ca/npsi/ctrl?action=rtdoc&an=11213134&lang=en
http://nparc.cisti-icist.nrc-cnrc.gc.ca/npsi/ctrl?action=rtdoc&an=11213134&lang=fr

Integrated High Temperature Piezoelectric Plate Acoustic Wave Transducers Using Mode Conversion

K.-T. Wu[1], M. Kobayashi[2] and C.-K. Jen[2]

[1] Department of Electrical and Computer Engineering, McGill University, Montreal, QC, H3A 2A7, CANADA

[2] Industrial Materials Institute, National Research Council Canada, Boucherville, QC, J4B 6Y4, CANADA

(cheng-kuei.jen@cnrc-nrc.gc.ca)

Abstract

Piezoelectric thick (>66μm) films have been directly coated onto aluminum (Al) substrates using a sol-gel spray technique. With a top electrode these films serve as integrated ultrasonic transducers (IUTs) which normally operate as thickness vibration longitudinal wave transducers. When such IUTs are located at the edges of the metallic plates, they can excite and detect symmetrical, anti-symmetric and shear horizontal types of PAWs using mode conversion methods. In 2mm thick Al plates two line defects of 1mm width and 1mm depth were clearly detected at temperatures up to 150°C in pulse-echo mode. Results indicated that for 2mm thick aluminum plates shear horizontal PAWs were the best for the line defect detection. Also the experimental results agree well with those obtained by a finite difference based method.

Keywords: Integrated ultrasonic transducer; nondestructive testing; structural health monitoring; plate acoustic waves; thick piezoelectric ceramic film; high temperature; mode conversion

I. INTRODUCTION

Structural health monitoring (SHM) [1, 2] is a major concern of the aerospace community when considering aging aircrafts whose growing maintenance costs can reduce their economic life extension. Also emerging new airplanes are increasingly required to be equipped with intelligence for improved diagnostics of the health condition of the critical parts and structures. Therefore, there are demands for miniaturized light weight integrated in-situ sensors and associated techniques for local and global (long distance) damage diagnostics [3]. In this investigation integrated ultrasonic transducers (IUTs) developed to generate and receive PAWs [4-6] which propagated many hundreds of mms along 2mm thick aluminum (Al) plates for global line defect detections will be developed. These IUTs will be fabricated at the end edges of the plates by a sol-gel spray technique [7-9]. They normally operate as thickness vibration longitudinal (L) modes transducers. Therefore mode conversions techniques [6, 10-12] will be used to use such IUTs to excite and detect symmetrical, anti-symmetrical and shear-horizontal (SH) types of PAWs. The operation temperature of these IUTs will be tested up to 150°C. The comparisons among these mode converted PAWs will be discussed.

II. TRANSDUCER FABRICATION

The sol-gel based sensor fabrication process to fabricate IUTs using metal substrates [7-9] consists of six main steps [7-9]: (1) preparing high dielectric constant lead-zirconate-titanate (PZT) solution, (2) ball milling of piezoelectric PZT powders to submicron size, (3) sensor spraying using slurries from steps (1) and (2) to produce the thin film, (4) heat treating to produce a solid composite (PZT/PZT) thin film, (5) corona poling to obtain piezoelectricity, and (6) electrode painting or spraying for electrical connections. Steps (3) and (4) are used multiple times to produce optimal film thickness for specified ultrasonic operating frequencies. Silver paste was used to fabricate top electrodes. For this study the top electrode size for IUT was chosen for the size and shape of the active area for PAW generation and receiving. Fig.1 shows a schematic of an IUT directly coated onto the end edge of an Al plate. On Al substrate the

measured electromechanical coupling and dielectric constant of the film are about 0.2 and 200, respectively.

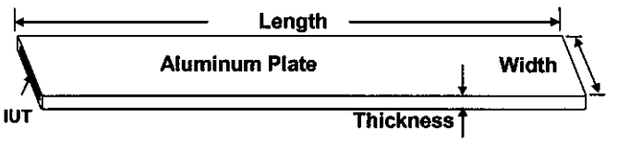

Fig. 1. Schematic of an IUT deposited onto the end edge of an Al plate.

III. MODE CONVERSION TECHNIQUE

The IUT shown in Fig.1 is, in principle, an L wave thickness vibration UT. However, when IUT deposited onto the end edge of a 2 mm thick Al plate as shown in Fig.1 this IUT will generate and receive symmetrical PAWs [4-6] due to the finite thickness of the plate.

Recently using mode conversion [10-12] L wave can be converted into shear (S) waves for nondestructive testing (NDT) applications. It is known that there exist shear vertical (S_V) and shear horizontal (S_H) waves in bulk materials [5, 6]. Here using IUTs the analogies of mode conversion from L wave to S_V and to S_H modes have been developed for the mode conversion from L like waves to anti-symmetrical and shear horizontal (SH) PAWs, respectively as shown in Figs.2 and 3. The mode conversion angles ϕ and θ shown in Figs.2 and 3, respectively will be discussed in the latter sections.

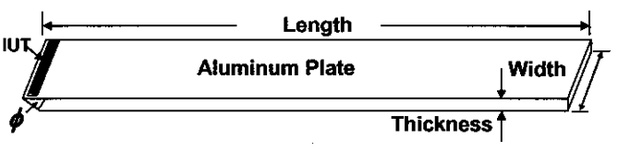

Fig. 2. Schematic of an IUT deposited onto the end edge of an Al plate to generate and receive anti-symmetrical PAWs.

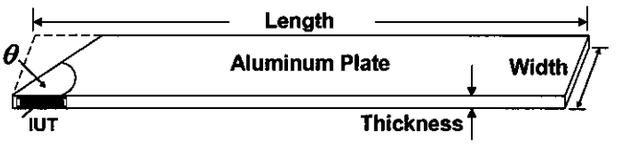

Fig. 3. Schematic of an IUT deposited onto the end edge of an Al plate to generate and receive shear-horizontal PAWs.

IV. ULTRASONIC PERFORMANCE

For SHM the ability of PAWs to detect defects in long distances is essential. Therefore the focuses in this section will be to (i) evaluate the propagation distance of symmetrical, anti-symmetrical and SH PAWs excited and received by the developed IUTs deposited onto the end edges of 2mm thick Al plates and (ii) the ability of these three types of PAWs to detect artificial line defects at room temperature and 150°C. In order to detect the defect locations pulse/echo mode is chosen although transmission mode can be used.

A. Symmetrical PAWs

Fig.4 shows the symmetrical PAWs ($S_{L,1}$) generated and received by the IUT shown in Fig.1 at 150°C in an 2mm thick, 50.8mm wide and 406.4mm long Al plate. The subscript 1 of the $S_{L,1}$ echo denotes the 1st round trip from the IUT location to the other edge of the plate. It means that $S_{L,1}$ has traveled a total distance of 812mm. The group velocity of the $S_{L,1}$ echo at the leading edge was about 5462m/s which is slower than that of the measured through Al plate thickness L wave velocity, V_L = 6364m/s. The calculated phase and group velocities for several low order symmetric and anti-symmetric modes are given in Fig.5. Fig.5 implies that $S_{L,1}$ consists of many lower order symmetrical modes. From the measured group velocity of 5462m/s it is believed that the main symmetrical mode contribution to the $S_{L,1}$ signal would be S^4 mode shown in Fig.5.

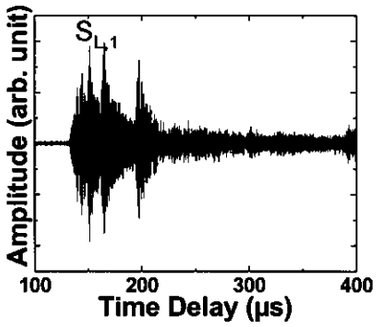

Fig. 4. Ultrasonic symmetrical PAW signals obtained in a 2mm thick Al plate using IUT shown in Fig.1 at 150°C.

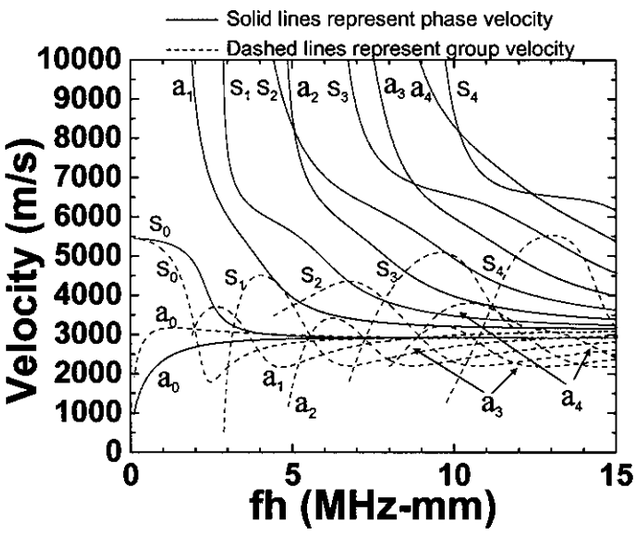

Fig. 5. Theoretical calculated phase and group velocities versus the product of PAW frequency, f, and plate thickness, h, curves for the first few symmetrical (S) and anti-symmetrical PAW modes in the 2mm thick Al plate.

To examine the long distance capability of SHM of the symmetrical PAWs two artificial line defects, D1 and D2 with 1mm depth and 1mm width were made onto the Al plate shown in Fig.1. D1 and D2 had length of 25.4mm and 50.8mm, respectively as shown in Fig.6. At 150°C the measured symmetrical PAWs are given in Fig.7. Fig.4 in which no line defects exist and Fig.7 in which two line defects present

clearly confirm that symmetrical PAWs can be used to perform SHM of defects at 150°C. In Fig.6 the two line defects were 146.3mm and 223.5mm away from the IUT.

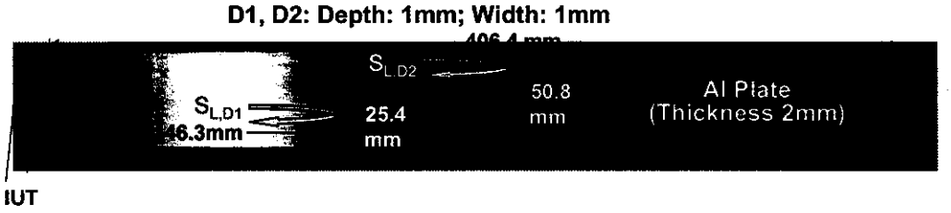

Fig. 6. Two artificial line defects, D1 and D2 were made onto a 2mm thick Al plate.

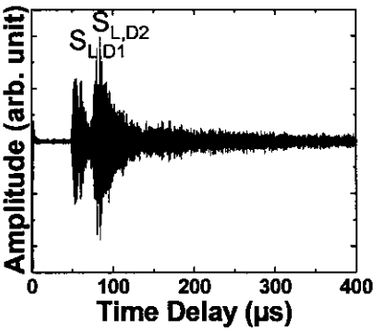

Fig. 7. Symmetrical PAW signals detecting two artificial line defects, D1 and D2 in a 2mm thick Al plate shown in Fig. 6 at 150°C.

B. Anti-symmetrical PAWs

In Fig.2 a 66μm thick PZT/PZT composite film IUT was coated on top of the Al plate. The chosen mode conversion angle ϕ using the analogy of bulk L wave to S_V for this configuration was 63.7° which was obtained from the phase matching angle [12] of the measured bulk L and S wave velocities of the Al plate. In a bulk Al sample the energy conversion rate from the bulk L wave to the S wave at this angle is 83.1%, which is only 0.02% smaller than the maximum conversion rate. Due to this mode conversion configuration the S_V becomes the anti-symmetrical modes (A_{SV}) because of the finite thickness of the Al plate. The A_{SV} is excited although the angle ϕ has not been optimized, because this is a plate (finite dimensions) configuration, the analogy of the bulk (infinite dimensions) material configuration is only

used for initial studies. In the future theoretical evaluation to obtain optimal conversion angle ϕ will be performed.

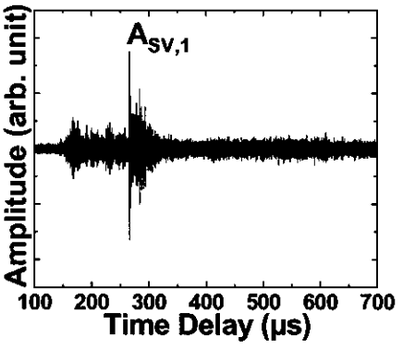

Fig. 8. Ultrasonic anti-symmetrical PAW signals obtained using IUT shown in Fig.2 at 150°C with mode conversion. The Al plate length was 406.4mm.

Fig.8 shows the reflected anti-symmetrical PAW $S_{AV,1}$ echoes at 150°C in the time domain. The subscript 1 of the $S_{AV,1}$ echo denotes the 1st round trip from the IUT location to the other edge of the plate. It indicates that $S_{AV,1}$ has traveled a total distance of ~812 mm. It is speculated that $S_{AV,1}$ may be composed of mainly the zeroth order anti-symmetrical PAW [4-6]. Since this Al plate supports multimode anti-symmetrical PAW propagation, some of the higher order modes having traveled faster than the zeroth order anti-symmetrical mode arrived earlier as shown in Fig.8.

To evaluate the defect detection ability of the current anti-symmetrical PAW configuration two line defects with dimensions and locations away from the IUT nearly identical to those (D1 and D2) for symmetrical PAWs shown in Fig.6 were created for the 2mm thick Al plate. The results showed that these two line defects could be detected but with much less SNR than that obtained from symmetrical PAW as shown in Fig.7.

C. Shear-horizontal (SH) PAWs

If the IUT is located at the edge indicated in Fig.3, SH PAWs [5, 6] can be produced and received using mode conversion. In Fig.3 the thickness of the PZT/PZT composite film was 90μm. For this configuration symmetrical PAW echoes traveled nearly 25.4mm and then converted to SH PAW modes and vice versa. For this configuration the chosen mode conversion angle θ using the analogy of bulk L wave to S_H was 61.7° which was calculated using the phase matching between measured extension mode velocity $S_{L,1}$ and the shear wave velocity of the Al plate. Similar to the mode conversion angle ϕ, θ will be optimized in the future study.

Using the IUT shown in Fig.3 the reflected SH PAWs echoes at 150°C without two line defects in time domain is given in Fig.9. After traveling nearly a distance of 813mm the center frequency of the $S_{H,1}$ echo was 6.3MHz. The subscripts 1 and 2 denote the 1st and 2nd round-trip echo, respectively. $S_{H,2}$ echo traveled a distance of 1.625m. Comparing with the PAW signals obtained for symmetrical and anti-symmetrical modes SH PAW echoes shows the highest SNR. Theoretical calculation results as shown in Fig.10 also reveal that $S_{H,1}$ echo mainly comes from the zeroth order SH PAW having the bulk shear wave velocity [5,6]. Also the group velocities of the higher order SH PAWs in the current configuration are slower that that of bulk shear wave velocity and that is why they arrived a little bit later than $S_{H,1}$ echo.

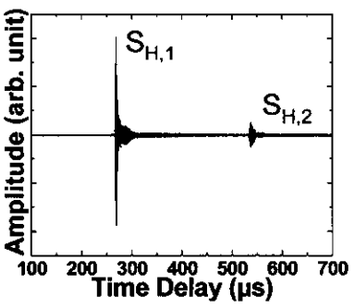

Fig. 9. Ultrasonic SH PAW signals obtained using IUT shown in Fig.11 on a 2mm Al plate at 150°C with mode conversion.

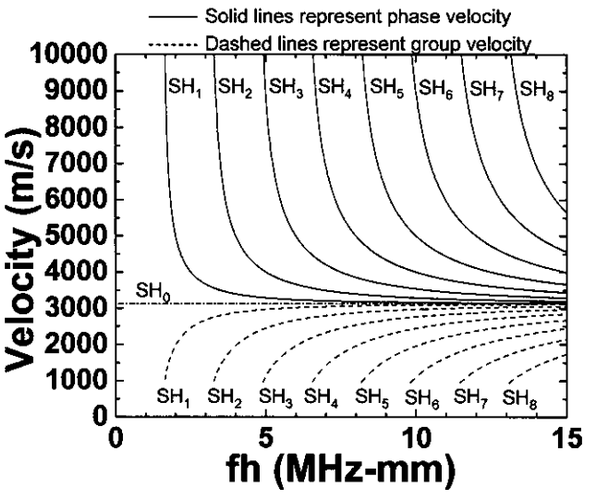

Fig. 10. Theoretical calculated phase and group velocities versus the product of PAW frequency, f, and plate thickness, h, curves for the first few SH PAW in the 2mm thick Al plate.

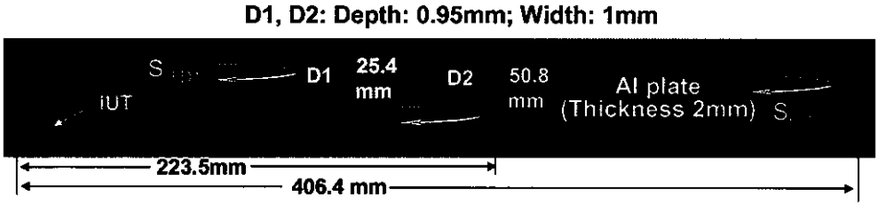

Fig. 11. One IUT coated directly onto side surface near the end edge of an Al plate as shown in Fig.3 with an angle of 61.7° to generate and receive SH PAW using mode conversion. Two artificial line defects, D1 and D2 were also made onto a 2mm thick Al plate.

Two line defects with dimensions and locations away from the IUT nearly identical to those (D1 and D2) for symmetrical PAWs shown in Fig.6 were created in the plate shown in Fig.11. At 150°C the reflected SH PAW signals are given in Fig.12. Fig.9 in which no line defects exist and Fig.12 in which two line defects present clearly confirm that SH PAWs can be used to perform SHM of line defects at 150°C. In the case shown in Fig.12 not only SH PAWs can clearly detect the defects which are 146.3mm and 223.5mm away from the IUT, but also travel to the end of the plate and return back to the IUT as indicated by the echo $S_{H,1}$ with good SNR. Therefore for the 2mm thick Al plate SH PAW showed the best SHM capability.

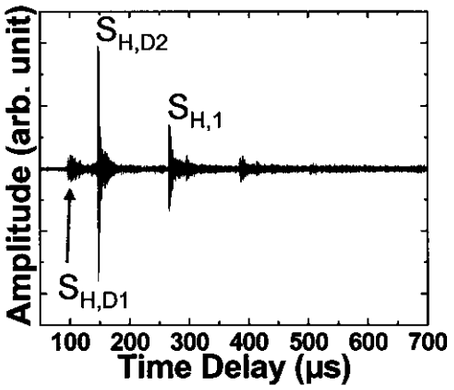

Fig. 12. SH PAW signals detecting two artificial line defects, D1 and D2 in a 2mm thick Al plate shown in Fig. 11 at 150°C.

C.1. In-situ ultrasonic measurement of an airframe structure using SH PAW

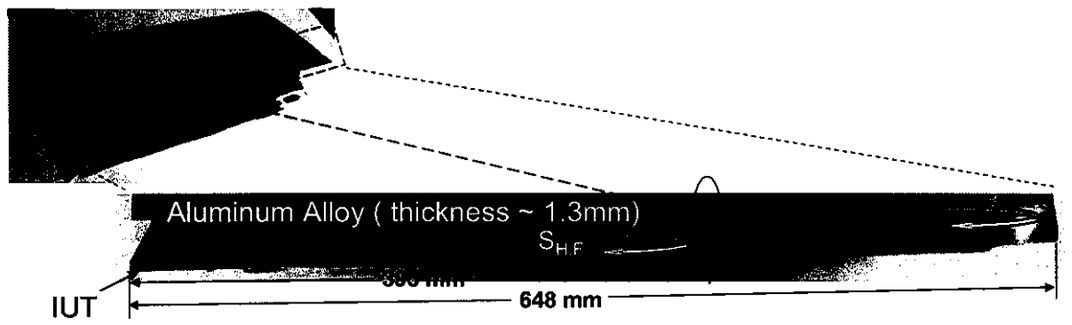

Fig. 13. One IUT coated directly onto side surface near the end edge of an Al horizontal stabilizer with an angle of 61.7° to generate and receive SH PAW using mode conversion. $S_{H,F}$ is SH PAW reflected from the location with a line-shape bolted joint underneath the frame and $S_{H,1}$ is that reflected from the end of the frame.

A Bombardier regional jet horizontal stabilizer shown in Fig.13 is then used as a test sample. The thickness of the Al frame is not uniform and ranges from 1.1 to 1.3 mm. At one edge of the Al plate indicated in Fig.13 an angle of $\theta = 61.7°$ is created to generate and receive SH PAW using mode conversion. An IUT consisting of 75μm PZT/PZT film and having a top silver paste electrode size of 12mm by 1mm was made

at the location indicated in Fig.13. The reflected SH PAW signals at room temperature are given in Fig.14. $S_{H,F}$ is SH PAW reflected from the location with a line-shape bolted joint underneath the frame and $S_{H,1}$ is that reflected from the end of the frame. Fig.14 demonstrates the capability of IUT to generate and detect SH PAW in a real airframe for possible SHM application.

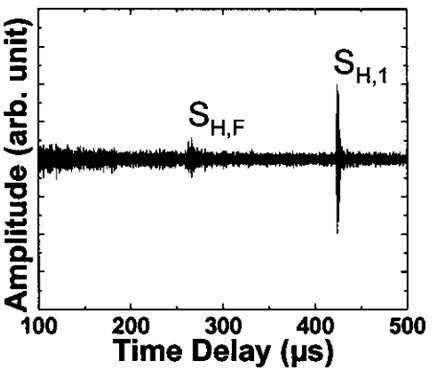

Fig. 14. Ultrasonic SH PAW signals obtained using IUT on an Al stabilizer shown in Fig.13 at room temperature.

V. Comparison Between Theoretical Calculations and Experimental Results

In order to reduce number of experiements to investigate the sensitivity of defect detection numerical simulation is valuable. Figs. 15(a) and 15(b) show the measured and numerically calculated results, respectively, in time domain at room temperature for the symmetrical PAW defect detection configuration shown in Fig.6. The numerical simulation used a commercial available software package (Wave3000 Pro, CyberLogic Inc., New York, NY) based on a finite difference method which solves the 3D visco-elastic wave equations. Comparing Figs.15(a) and 15(b) a good agreement between the experimental obtained and numerically calculated signals in signal bandwidth and time delay has been achieved. The simulated results took the computation time of 21 days using a computer equipped with 64-bit operation system and 16G memories. Also the measured and numerically simulated results in time domain and at room temperature for the SH PAW defect monitoring configuration shown in Fig.11 are shown in Figs.16(a) and 16(b), respectively. Also a good agreement between the results shown in Figs.16(a) and 16(b) can be seen. The

numerical simulation for Fig.16(b) took 21 days of calculation. It is noted that because of the texture of the plates the measured time delay is slightly less than the calculated one in which the textures are not considered. Such simulation approach will be used in the future for the detection sensitivity evaluation of cracks using the symmetrical, anti-symmetrical and SH PAW configurations presented in this investigation.

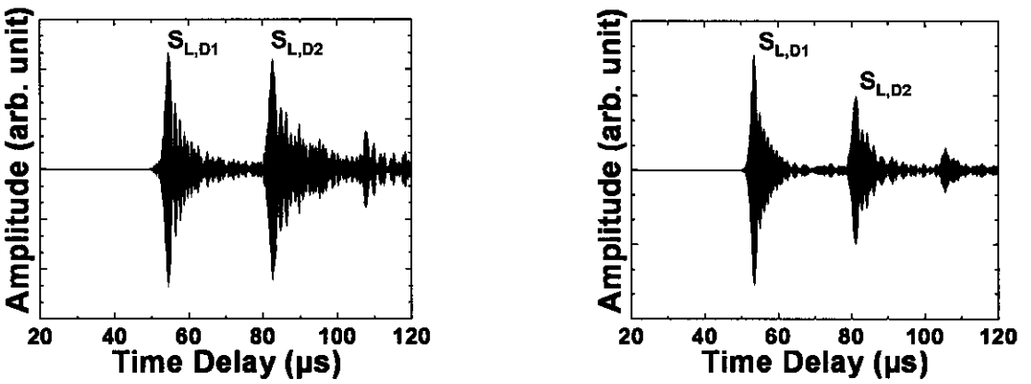

Fig. 15. (a) Measured and (b) numerically calculated symmetric PAW signals in time domain at room temperature in the Al plate as shown in Fig.6.

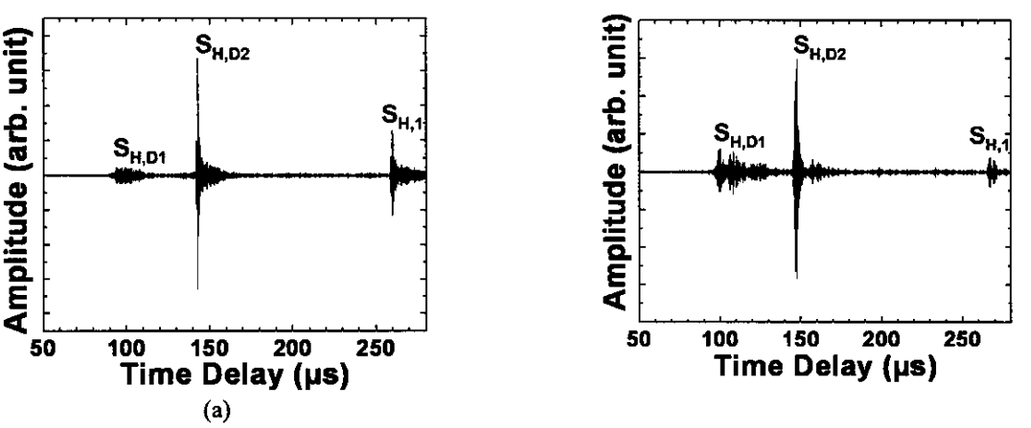

Fig. 16. (a) Measured and (b) numerically calculated SH PAW signals in time domain at room temperature in the Al plate as shown in Fig.11.

VI. CONCLUSIONS

Piezoelectric thick (>66μm) PZT/PZT composite films were directly coated onto Al plates using a sol-gel spray technique. With a top line electrode these films served as integrated ultrasonic transducers (IUTs) which normally operate as thickness vibration L wave transducers. When an IUT is fabricated at the end edge of the Al plate as shown in Fig.1, it can excite and detect symmetrical PAW due to the finite thickness of the Al plate. If an IUT is coated onto the top edge at the end of the Al plate as shown in Fig.2 L waves will be converted into S_V wave due to mode conversion. It becomes then the anti-symmetric PAW due to finite Al thickness. The chosen mode conversion angle ϕ using the analogy of bulk L wave to S_V for this configuration was 63.7° which was obtained from the phase matching angle [12] of the measured bulk L and S wave velocities of the Al plate. It is not the optimal one and will be studied further in the future. When an IUT is deposited onto the side edge at the end of the Al plate as shown in Fig.3, the IUT will generate the extension wave in the beginning and then converted to SH PAW in the Al plate at the slanted edge. The selected slanted angle was 61.7° which was not optimized and this optimal angle will be studied in the future as well. In 2mm thick Al plates two line defects of 1mm width and 1mm depth were clearly detected at temperatures up to 150°C in pulse-echo mode for using symmetrical, anti-symmetrical and SH PAWs. Results indicated that for 2mm thick aluminum plates SH PAWs were the best for the line defect detection. SH PAW propagation was also demonstrated on a real regional jet horizontal stabilizer made of Al plate of thicknesses ranging from 1.1mm to 1.3mm. The results indicated that SH PAWs may be used for SHM purposes. Also the experimental results agreed well with those obtained by a finite difference based method which solves the 3D visco-elastic wave equations.

ACKNOWLEDGMENT

Financial support of K.-T. Wu from Natural Sciences and Engineering Research Council of Canada is acknowledged.

REFERENCES

[1] M.V. Gandhi and B.S. Thompson, *Smart Materials and Structures*, London: New York, Chapman & Hall, 1992.

[2] J.-B. Ihn, and F.-K. Chang, "Ultrasonic Non-destructive Evaluation for Structure Health Monitoring: Built-in Diagnostics for Hot-spot Monitoring in Metallic and Composite Structures", Chapter 9 in *Ultrasonic Nondestructive Evaluation Engineering and Biological Material Characterization*, T. Kundu, Ed. Florida:CRC Press, 2003.

[3] A.S. Birks, R.E. Green, Jr. and P. McIntire, *Nondestructive Testing Handbook*, 2nd ed., vol.7: Ultrasonic Testing, ASNT, 1991.

[4] I.A. Viktorov, *Rayleigh and Lamb waves*, New York: Plenum, 1967.

[5] G.S. Kino, *Acoustic Waves, Devices, Imaging & Analog Signal Processing*, New Jersey: Prentice-Hall, 1987.

[6] B.A. Auld, *Acoustic Fields and Waves in Solids*, vol.1 and 2, John Wiley & Sons, New York, 1973.

[7] D. Barrow, T.E.. Petroff, R.P. Tandon, and M. Sayer, "Chracterization of thick lead-zirconate titanate films fabricated using a new sol gel process," *J. Apply. Phys.*, vol. 81, pp. 876-881, 1997.

[8] M. Kobayashi and C.-K. Jen, "Piezoelectric thick bismuth titanate/PZT composite film transducers for smart NDE of metals," *Smart Materials and Structures*, vol. 13, pp. 951-956, 2004.

[9] C.-K. Jen and M. Kobayashi, "Integrated and flexible high temperature piezoelectric ultrasonic transducers", Chapter 2 in *Ultrasonic and Advanced Methods for Nondestructive Testing and Material Characterization*, C.H. Chen, Ed. New Jersey: World Scientific Publishing, 2007, pp.33-55.

[10] M.O. Si-Chaib, H. Djelouah and M. Bocquet, "Applications of ultrasonic reflection mode conversion transducers in NDT," *NDT&E Int'l*, vol. 33, pp. 91-99, 2000.

[11] C.-K. Jen, Y. Ono and M. Kobayashi, "high temperature integrated ultrasonic shear wave probes," *Applied Phys. Lett.*, vol. 89, pp. 183506_1-3, 2006.

[12] Y. Ono, C.-K. Jen and M. Kobayashi, "High temperature integrated ultrasonic shear and longitudinal wave probes," *Review of Scientific Instruments*, vol. 78, pp. 0249031-5, 2007.